Desalination and Water Treatment

Enhancement of poly(phenyl sulfone) membranes with ZnO nanoparticles

Qusay F. Alsalhy [a], Jamal M. Ali [a], Ali A. Abbas [b], Ali Rashed [c], Bart Van der Bruggen [c] & Stefan Balta [d]

[a] Department of Chemical Engineering, Membrane Technology Research Unit, University of Technology, Alsinaa Street 52, Baghdad, Iraq Phone: Tel. +964 7901730181

[b] Department of Pumping Engineering, Technical College, Foundation of Technical Education, Al-Musaib, Babylon, Iraq

[c] Department of Chemical Engineering, KU Leuven, Belgium

[d] Department of Environmental and Material Engineering, Dunarea de Jos University, Galati, Romania

PLEASE SCROLL DOWN FOR ARTICLE

Enhancement of poly(phenyl sulfone) membranes with ZnO nanoparticles

Qusay F. Alsalhy[a,*], Jamal M. Ali[a], Ali A. Abbas[b], Ali Rashed[c], Bart Van der Bruggen[c], Stefan Balta[d]

[a]*Department of Chemical Engineering, Membrane Technology Research Unit, University of Technology, Alsinaa Street 52, Baghdad, Iraq*
Tel. +964 7901730181; email: qusayalsalhy@uotechnology.edu.iq
[b]*Department of Pumping Engineering, Technical College, Foundation of Technical Education, Al-Musaib, Babylon, Iraq*
[c]*Department of Chemical Engineering, KU Leuven, Belgium*
[d]*Department of Environmental and Material Engineering, Dunarea de Jos University, Galati, Romania*

ABSTRACT

In this work, poly(phenyl sulfone) (PPSU) membranes were prepared by diffusion-induced phase inversion method in N-methyl-pyrrolidone using different concentrations of ZnO nanoparticles as additives. The main objective of this work is to evaluate the performance of the PPSU membranes with ZnO nanoparticles. The concentrations of ZnO were 0, 0.01, 0.015, 0.02, 0.025, and 0.03 wt.%. The effect of the ZnO nanoparticles on the characteristics of PPSU membranes was investigated with scanning electron microscopy and atomic force microscopy observations, contact angle measurement, nanofiltration experiments, and observations of solute rejection. It was found that the cross-section structure of the membrane changes from a finger-like and sponge-like structure formed near the support and top layers, respectively, to fully sponge-like structure with increase of ZnO concentration up to 0.025 wt.%. The mean pore size and mean roughness of the PPSU/ZnO membranes increased with the ZnO concentration. The membrane hydrophilicity increases due to the addition of ZnO nanoparticles. The flux of the PPSU membranes with 0.025 wt.% ZnO as additives enhanced from 76 to 107 $(L\,m^{-2}\,h^{-1}\,bar^{-1})$ with no significant change in solute rejection.

Keywords: Membranes; Nanofiltration; PPSU; ZnO; Nanoparticles

1. Introduction

Poly(phenyl sulfone) (PPSU) is one of the most preferred polymers in a wide range of polymers used for the preparation of the membranes, due to the superior combination of high performance properties, including an excellent thermal stability, outstanding toughness, and good environmental stress cracking resistance [1–3]. However, few studies have been done using PPSU membranes for nanofiltration applications due to the undesirably hydrophobic by nature, thus, PPSU membranes are strongly liable to fouling by organics such as ethyl acetate, *n*-hexane, toluene, diethyl ether, isopropanol, and acetone [1,2]. Darvishmanesh et al. prepared nanofiltration membranes at different PPSU

*Corresponding author.

compositions with three types of solvent such as, dimethylacetamide (DMA), N-methyl-2-pyrrolidone (NMP), and a mixture of dimethylformamide (DMF) and NMP using the phase inversion method [1,2].

Among the recent methods proposed to improve the membrane properties such as anti-fouling, permeability, solute rejection, morphology, hydrophilicity and mechanical properties, and the addition of inorganic nanoparticles to the membrane dope solution [4–7]. Several types of nanoparticles have been used to enhance the membranes performance, such as silica (SiO$_2$) [8], Titanium dioxide (TiO$_2$) [4,5,7], alumina (Al$_2$O$_3$) [9,10], zirconia (ZrO$_2$) [11–13], and CdS [14]. Very few studies have been done regarding the use of ZnO nanoparticles with polymeric membranes [15–17]. For example, Balta et al. [15] prepared novel flat-sheet nanofiltration using ZnO nanoparticles in order to enhance the performance of the membrane. They found a significant improvement compared to the neat membranes in terms of permeability, dye rejection, and fouling resistance by adding ZnO nanoparticles even in small concentrations. Shen et al. [16] prepared polyethersulfone (PES) membranes with different compositions of ZnO nanoparticles in casting solution by using phase inversion method. It was found that, with the increase of ZnO concentration the contact angle decreases. The porosity of ZnO/PES membrane is improved by adding ZnO. The flux of ZnO/PES membrane exhibits an improvement of 254% in comparison to the neat PES membrane, whereas there is no significant effect of ZnO on the solute rejection. Hong and He [17] modified polyvinylidene fluoride (PVDF) microfiltration membranes by adding ZnO particles in casting solution. The PVDF membrane hydrophilicity was improved with the addition of ZnO particles. Also, they found maximum pure water flux of the membrane with addition of 0.005 wt.% ZnO particles.

The originality of this work is in the preparation of PPSU membranes by using nano-ZnO as inorganic additive to enhance the performance of nanofiltration technology. The performance of the membranes was conducted in terms of pure water permeation flux and dye rejection, whereas, the resultant membrane structure was studied by using scanning electron microscope (SEM) and atomic force microscope (AFM). In addition, the hydrophilicity of the membrane surface was investigated by using the contact angle measurement.

The use of ZnO nanoparticles is applied for the first time in this study to enhance PPSU membranes, as an alternative to the PES membranes studied by Balta et al. and Shen et al. [15,16]. This polymer has been demonstrated to have excellent properties in pervaporation [18]; in this paper, it is hypothesized that

ZnO-enhanced PPSU membranes may have a good performance in nanofiltration as well.

2. Experimental work

2.1. Materials

PPSU, Radel R-5000 with average $M_w = 50$ KDa, and specific gravity = 1.28 was provided by Solvay Advanced Polymers (Belgium). NMP, 99.5% and ZnO nanoparticles were used as the polymer solvent and additive, respectively, and were purchased from Sigma–Aldrich (St. Louis, MO). The support layer (Viledon FO2413) used for the manufacturing of PPSU membrane was obtained from Freudenberg (Weinheim, Germany). The organic compound used as a solute, C$_{45}$H$_{32}$N$_{10021}$S$_{6.6}$Na and Fw Direct red 80 ($M_w = 1373.09$), was purchased from ACROS Organics (Belgium).

2.2. Membrane preparation

Pure PPSU membranes were prepared using phase inversion induced by immersion precipitation. PPSU cast from 22 wt.% PPSU in NMP was used as the polymer matrix. A ZnO nanoparticle was dissolved in the corresponding weight of NMP by magnetic stirring for 3 h at room temperature. Five different concentrations of ZnO nanoparticles were used: 0.01, 0.015, 0.02, 0.025, and 0.03 wt.%. Then, the polymer was added to the solution, which was stirred for 24 h at 40℃ until formation of a homogeneous solution. After that, the films were cast with 250 µm thickness using a filmograph (K4340 Automatic Film Applicator, Elcometer) in an atmosphere with controlled relative humidity on non-woven polyester as a support layer (FO2413 polyester, air permeability at 2 mbar: 150 dm^3/m^2 s). Prior to the casting, the support layer was wetted with NMP to prevent the polymer solution of intruding in the pores of the support layer. The prepared films were immersed in a deionized water bath at 20℃ for precipitation. The membrane was kept in distilled water for 24 h to remove the residual solvent, and stored wet. For each polymer solution composition, three identical membrane sheets were made and tested to obtain an average value of flux and solute rejection.

2.3. Characterization of the membrane surface

2.3.1. Contact angle measurement

A contact angle measuring system DSA 10 Mk2 (Krüss, Germany) was used to measure the water contact angle of the dry flat homogeneous PPSU/ZnO

membranes. The average contact angle for distilled water was determined in a series of five measurements for each of the different membrane surfaces.

2.3.2. Scanning electron microscopy

SEM measurements were used to visualize cross-section and top surface characteristics of the membranes. SEM images were made with a TESCAN VEGA3 SB instrument (EO Elektronen-Optik-Service GmbH, Germany) with an accelerating voltage of 30 keV. Cross-sections were prepared by fracturing the membranes in liquid nitrogen. The SEM images of the cross-section and outer surfaces of the membrane were observed at various magnifications.

2.3.3. Atomic force microscope

Each flat-sheet membrane was subjected to extensive surface analysis using an AFM of Angstrom Advanced Inc. (USA), model AA3000, in contact mode with a suitable silicon tip. Measurements included an assessment of the topography (the rise and fall of the sample surface), the lateral force (friction forces between tip and sample, which causes the torsion of the cantilever and can be reflected by the photodetector's left–right signal), and deflection (cantilever flexes because of the rise and fall of sample topography and the amount of this deflection can be reflected by the photodetector's up–down signal). By using IMAGER 4.31 software, a statistical pore size distribution was established for the outer surfaces of each flat-sheet membrane.

2.4. Permeation flux and dye rejection

The pure water permeation flux and dye rejection studies of the membranes were conducted using dead-end filtration experiments. Three membrane coupons of the same membrane sheet for six membranes of each type were tested. All experiments were performed at a transmembrane pressure of 6 bar and feed solution temperature of 25℃ in dead-end mode with a Sterlitech HP4750 Stirred Cell. The effective membrane area was 14.6 cm^2. The volume of the solution was 250 ml. Permeate was collected in a graduated cylinder for a time interval until steady state. Pure water permeability (PWP) was obtained as follows:

$$PWP = \frac{V}{t \cdot A \cdot P} \tag{1}$$

where PWP is the PWP of the membrane (l/(m^2 h bar)), V is the volume collected (l), t is permeate collected time (h), (P) is the transmembrane pressure, and A is the membrane surface area (m^2).

A Shimadzu UV-1601 double beam spectrophotometer was used to determine the concentration of dyes. An aqueous solution of dye (Fw Direct red 80; $M_w = 1373.09$) with a concentration of 20 mg l^{-1} was used for the measurement of solute rejection. The rejection R (%) of the dissolved dyes was calculated as follows:

$$R\ (\%) = \left(1 - \frac{C_p}{C_f}\right) \times 100 \tag{2}$$

where C_f and C_p are the dye concentration in feed and permeate solution, respectively. The concentration of dye was determined based on absorbance in a UV-spectrophotometer at a wavelength of 528.5 nm [19].

3. Results and discussion

3.1. Effect of ZnO nanoparticles on PPSU membranes structure

Fig. 1 shows the SEM images of the top surface of the membrane prepared from neat PPSU and the PPSU membrane prepared with different concentrations of ZnO nanoparticles (i.e. 0, 0.01, 0.015, 0.02, 0.025, and 0.03 wt.%) in the casting solution. It can be noticed that there is no significant effect of the ZnO nanoparticles in the casting solution on the top surface structure of the PPSU membrane, except the formation of aggregates of ZnO nanoparticles spreading on the top surface of the membrane. Balta et al. [15] reported that the neat PES membrane's top surface was similar to that of the same membranes after addition of different concentrations of the ZnO nanoparticles to the dope solution.

Cross-sectional SEM images of prepared PPSU membranes with and without addition of different concentrations of ZnO nanoparticles in the PPSU casting solution are shown in Fig. 2. It can be noticed that a finger-like layer is formed near the polyester support layer, whereas a sponge-like layer is formed near the top surface of the cross-section of the membrane prepared from neat PPSU as shown in Fig. 2(a). In Fig. 2(b) it can be seen that the size and abundance of finger-like macrovoids decreased, while the sponge-like structure increased with addition of 0.01 wt.% ZnO nanoparticles in the casting solution. A further increase of the concentration of ZnO nanoparticles in the casting solution to 0.015 wt.% results in a thin finger-like structure; the sponge-like structure becomes more pronounced near the top surface, as shown in Fig. 2(c). A further increase in the concentration of ZnO nanoparticles in the casting solution to 0.02 and 0.025 wt.% changed the structure of the PPSU membranes to a fully sponge-like structure,
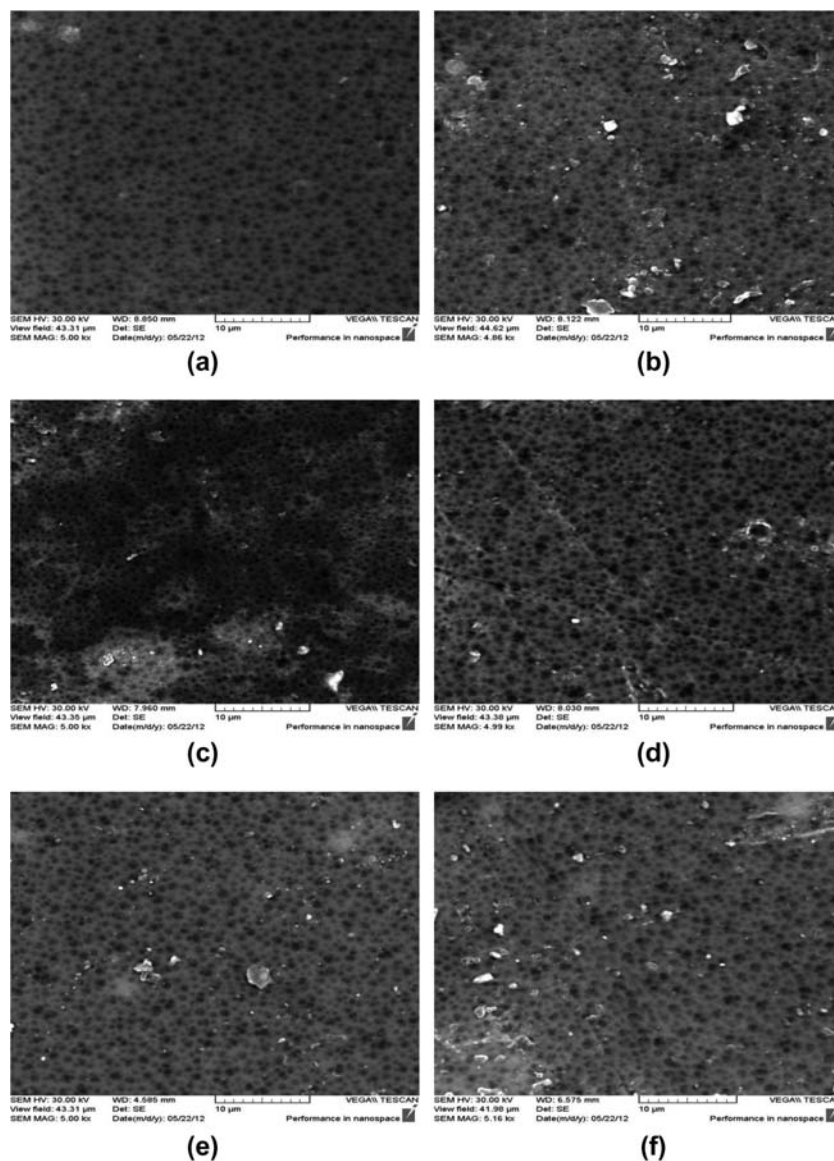
Fig. 1. SEM images of the surface of the PPSU membranes at different ZnO concentrations: (a) 0 wt.% ZnO; (b) 0.01 wt.% ZnO; (c) 0.015 wt.% ZnO; (d) 0.02 wt.% ZnO; (e) 0.025 wt.% ZnO; and (f) 0.03 wt.% ZnO.

as shown in Fig. 2(d) and (e). This phenomenon is attributed to the delayed liquid–liquid demixing process between the polymer solution and the non-solvent (water) due to the presence of ZnO nanoparticles in polymer solution. Yang et al. [20] reported that the macrovoids grow and become run-through at low nanoparticles concentration and are suppressed at higher nanoparticles concentration. This phenomenon indicates that the addition of ZnO nanoparticles in polymer casting solution has a significant effect on the membrane structure. Moreover, using 0.03 wt.% ZnO nanoparticles to the casting solution led to change the structure of the PPSU membrane to a finger-like struc-

ture in the entire cross-section of the membrane. This phenomenon is attributed to the reduction of the dispersion rate of nanoparticles, because the ZnO nanoparticle possesses high surface energy, which leads to the agglomeration of nanoparticles, which results in an increase of the non-solvent (water) exchange rate with NMP in the polymer solution. Therefore, it can be conclude that the mechanism of composite membrane is changed significantly by the addition of nanoparticles in polymer casting solution. Fig. 3 shows three-dimensional AFM images of the top surfaces of the PPSU membranes prepared at different ZnO concentrations in the casting solution. In these images, the darkest
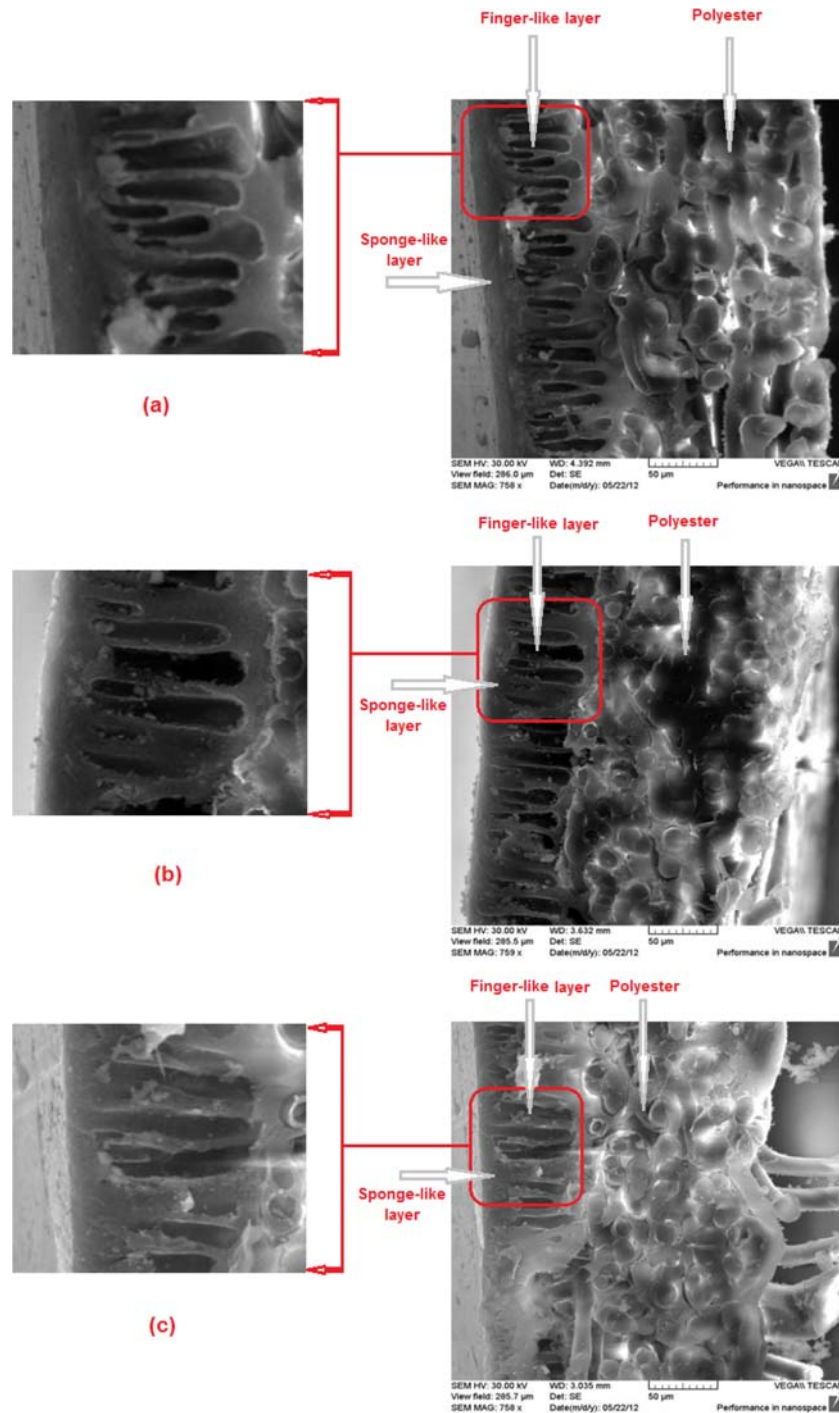
Fig. 2. SEM images of the cross-section of the PPSU membranes at different ZnO concentrations: (a) 0 wt.% ZnO; (b) 0.01 wt.% ZnO; (c) 0.015 wt.% ZnO; (d) 0.02 wt.% ZnO; (e) 0.025 wt.% ZnO; and (f) 0.03 wt.% ZnO.

regions are valleys or pores and the bright regions are the highest points or nodules. An important observation that can be seen in Fig. 3 is the different shapes of nodules in the top surface of PPSU membranes prepared at different ZnO nanoparticles. It can be noticed

that the nodular aggregates are merged together and formed a number of string-like structures with addition of ZnO nanoparticles up to 0.025 wt.%. A further increase of the ZnO concentration results in nodular aggregates in the shape of spheres dispersed on the
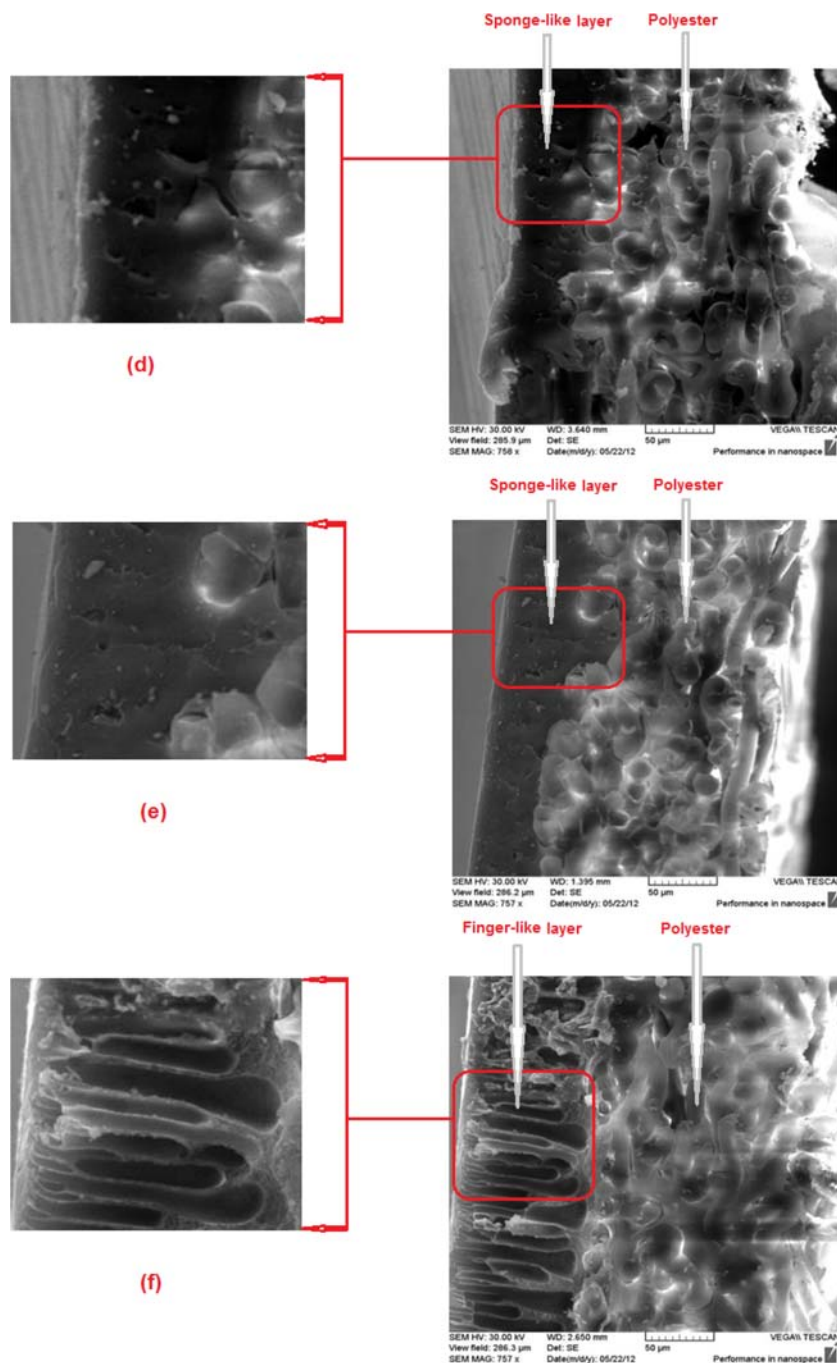
Fig. 2. (*Continued*)

membrane surface. Table 1 shows the mean pore size, the mean roughness (R_a) (the mean value of the surface relative to the center plane), the root mean square of Z values (R_{ms}), and maximum roughness (R_{max}) (vertical distance between the highest peaks and the lowest valleys) of the top surfaces of the PPSU membranes as evaluated over an area of $1 \times 1\,\mu m^2$. It can be noticed that the mean roughness of the PPSU membranes

increases with increase of the fraction of ZnO nanoparticles. This is attributed to the size of ZnO lumps formed on the surface of the membranes. Sotto et al. [21] reported that the size of the TiO_2 clusters formed as a result of agglomeration of nanoparticles was the main reason for the increase of the mean roughness of the PES membranes. On the other hand, the presence of the ZnO nanoparticles in the casting solution results in
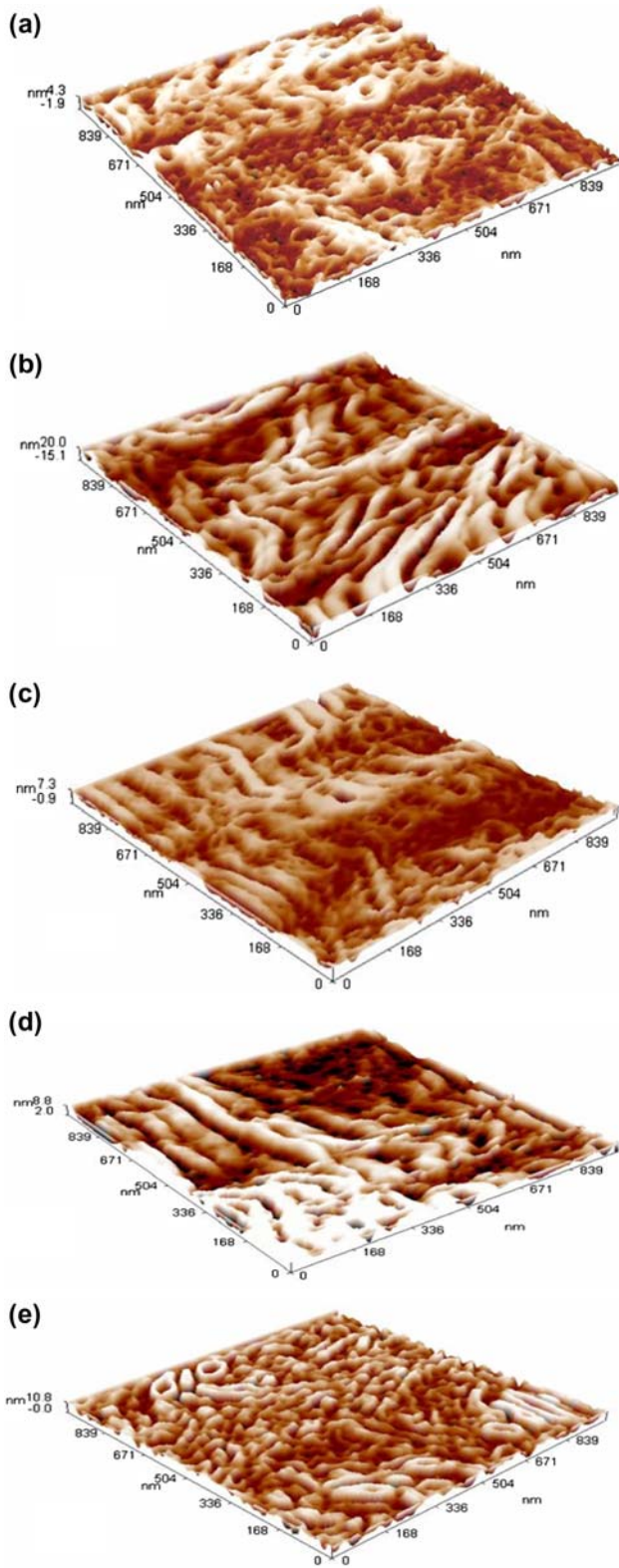
Fig. 3. Three-dimentional AFM images of the PPSU hollow fiber membranes: (a) ZnO 0 wt.%; (b) ZnO 0.01 wt. %; (c) ZnO 0.015 wt.%; (d) ZnO 0.025 wt.%; and (e) ZnO 0.03 wt.%.

Table 1
Mean pore size and mean roughness of the PPSU membranes

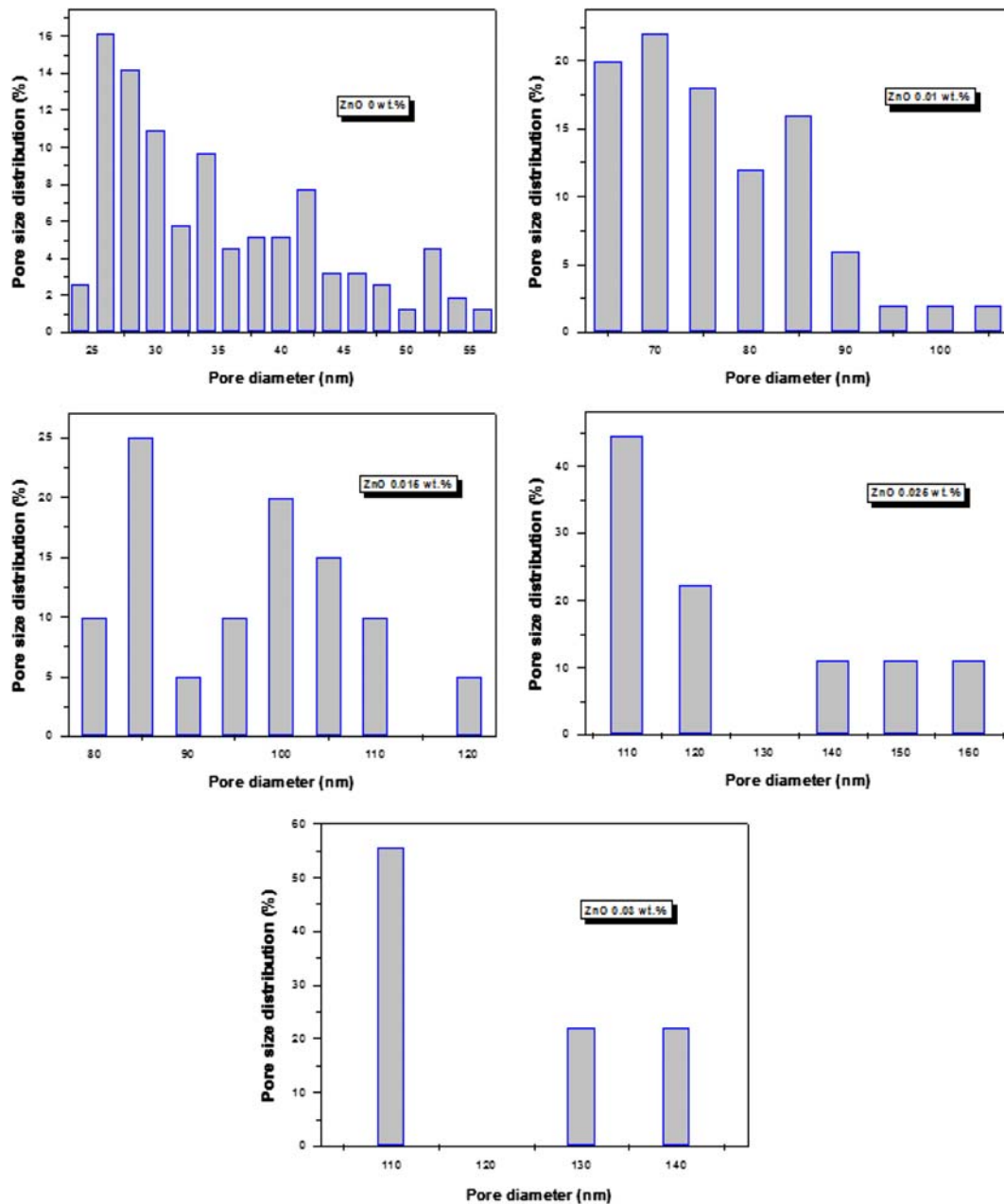| ZnO concentration (%)	Mean pore size (nm)	Top surface roughness ($1 \times 1 \, \mu m^2$)		
		Mean roughness (R_a) (nm)	The root mean square of Z values (R_{ms}) (nm)	Maximum roughness (R_{max}) (nm)
0	34.07	1.4	1.64	6.11
0.01	74.13	1.46	1.69	6.23
0.015	93.41	1.48	1.72	6.28
0.02	Not measured	–	–	–
0.025	120.43	2	2.28	6.81
0.03	116.12	2.46	2.88	10.7

Fig. 4. Pore size distributions of PPSU/ZnO membranes with: 0 wt.% ZnO; 0.01 wt.% ZnO, 0.015 wt.% ZnO, 0.025 wt.% ZnO, and 0.03 wt.% ZnO.

delayed liquid–liquid demixing during the preparation of the membrane, which in turn increases the pore size of the membrane. In Table 1, it can be noticed that the increase in mean pore size with addition of ZnO accompanied an increase in the mean roughness of the membrane surface. This phenomenon was in agreement with what was reported in the literature [21–24]. For example, Rajesh et al. [24] reported that a change in the mean roughness of the membrane surface is proportional to the change in the pore size. Regarding the

effect of the ZnO concentration on the pore size distribution, different pore sizes were obtained in top surfaces depending on the ZnO nanoparticles used in the PPSU casting solution. These results are evident from the pore size distribution and cumulative pore size distributions as shown in Fig. 4 and Fig. 5. It is clear that there is a significant effect of the ZnO concentration on the pore size distribution of the top surface of PPSU membranes. With an increase of ZnO nanoparticles to the PPSU casting solution, the pore size distribution
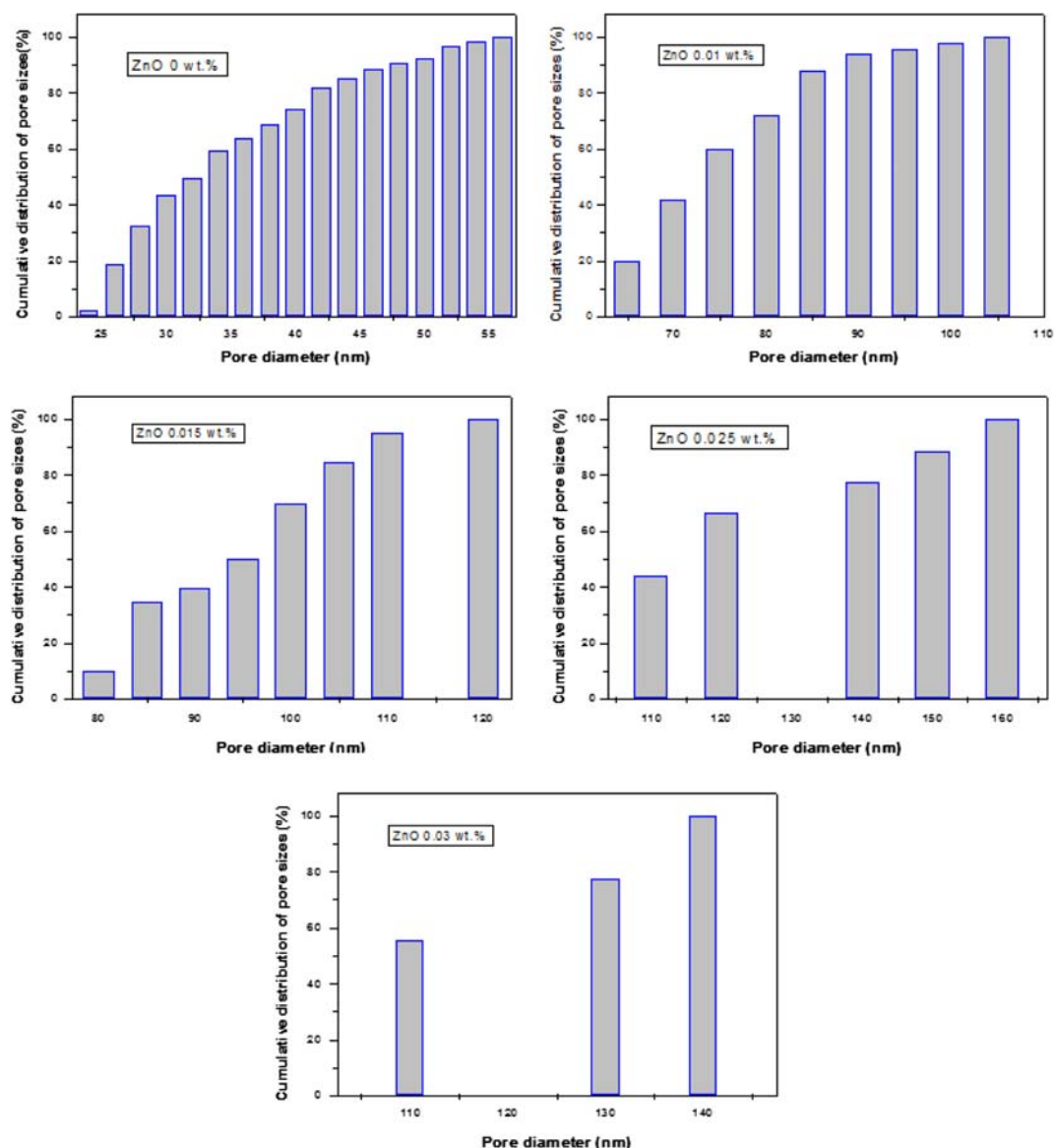
Fig. 5. Cumulative distributions of pore sizes measured from AFM images of the top surfaces of the PPSU membranes prepared at different ZnO concentrations.

and cumulative distributions of pore sizes shifted to the right in comparison to the neat PPSU membrane. The pore size distribution becomes narrower with an increase of ZnO nanoparticles in the casting solution. This can be explained by the variation in the exchange rate between the solvent in the polymer solution and the non-solvent (water) in the coagulation bath.

3.2. Effect of ZnO nanoparticles on the hydrophilicity of the PPSU membranes

The contact angles of PPSU membranes with different concentrations of ZnO nanoparticles (i.e. 0, 0.01,

0.015, 0.02, 0.025, and 0.03 wt.%) are shown in Fig. 6. It can be noticed that the membrane hydrophilicity is improved by addition of ZnO nanoparticles in the PPSU casting solution. The contact angle of the PPSU membranes decreased from 78.1 for neat PPSU membrane to 48.4 for PPSU membranes prepared from 0.03 wt.% ZnO nanoparticles. According to the strong alliance between the nanoparticles and water, the addition of ZnO nanoparticles to the PPSU casting solution can decrease the contact angles and improve the hydrophilicity of the membrane. This is due to the hydrophilic character of the ZnO nanoparticles in the membrane structure [15].
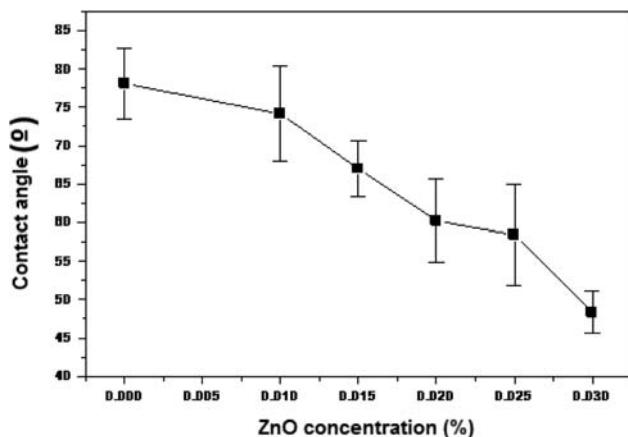
Fig. 6. Contact angles measured for neat PPSU and PPSU membranes at different ZnO nanoparticle concentrations in casting solution.

3.3. Effect of ZnO nanoparticles on the performance of PPSU membranes

Fig. 7 shows the effect of different ZnO nanoparticles concentrations in the PPSU casting solution on the pure water permeability of the PPSU membranes. The pure water permeability was 76 $(L\,m^{-2}\,h^{-1}\,bar^{-1})$ for the neat PPSU membrane, whereas addition of ZnO nanoparticles in casting solution results to increase of pure water permeability from 78 $(L\,m^{-2}\,h^{-1}\,bar^{-1})$ for the PPSU membrane prepared from 0.01 wt.% ZnO nanoparticles to 107 $(L\,m^{-2}\,h^{-1}\,bar^{-1})$ for PPSU membrane prepared from 0.025 wt.% ZnO nanoparticles in the casting solution. This phenomenon is attributed to the change of the PPSU structure from a finger-like to a sponge-like structure and also due to the increase of hydrophilicity due to the addition of ZnO nanoparticles in casting solution, as shown in Figs. 1 and 3 and discussed in
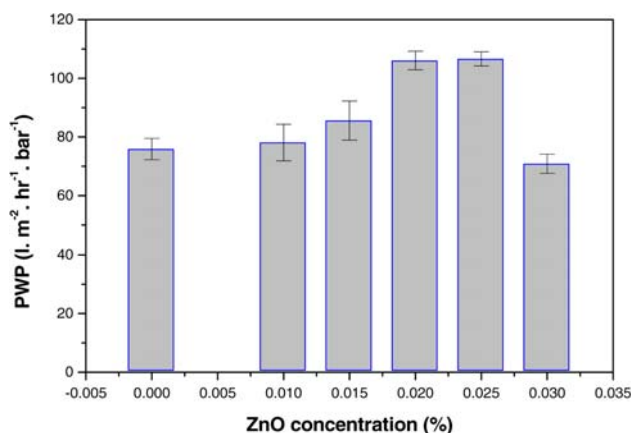
Sections 3.1 and 3.2, respectively. From the literature, it was reported that the improvement of the membrane structure and the increase of the hydrophilicity of the membrane due to the addition of nanoparticles were the main reason for enhancement of the membrane performance [15,16,25]. On the other hand, addition of ZnO nanoparticles up to 0.025 wt.% increases the pore size of the PPSU membrane, which in turn increases the permeation flux, as shown by the data in Table 1. Also from Fig. 7, it can be noticed that there is no significant improvement in the pure water fluxes of the PPSU membranes with increase of ZnO nanoparticles from 0.02 to 0.025 wt.% in the casting solution. This is due to the similar structure (i.e. sponge-like structure) of the two membranes [see Fig. 2(d) and (e)]. A further increase in the concentration of ZnO nanoparticles up to 0.03 wt.% results in a decrease of the pure water permeability. This phenomenon is attributed to the structural change of the PPSU membrane from a sponge-like to finger-like structure and the reduction of the mean pore size as shown in Table 1, Fig. 2(e) and (f). It is worth to mention that the effect of membrane structure on the pure water permeability of the PPSU membranes overcomes the effect of the membrane hydrophilicity measured by the contact angle of the membrane as shown in Fig. 3. On the other hand, Shen et al. [16] reported that when the composition of ZnO in casting solution increases to 0.4 g, the aggregation of ZnO nanoparticles is very influential that may make some pores blocked, which makes the water flux strongly decline.

Fig. 8 shows the effect of ZnO nanoparticles in the casting solution on the *Direct red 80* rejection by the PPSU membranes. It can be noticed that the rejections deceased from 99% for the neat PPSU

Fig. 7. PWP $(l\,m^{-2}\,h^{-1}\,bar^{-1})$ for neat PPSU and PPSU at different ZnO concentrations in casting solution.
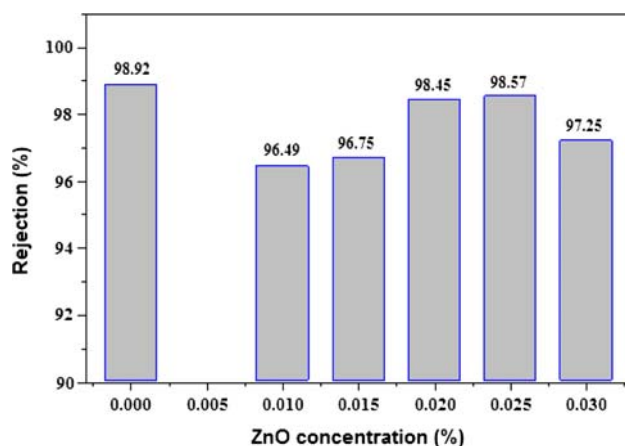

Fig. 8. Fw Direct red 80 rejection (%) of the neat PPSU and PPSU membranes at different ZnO concentrations in casting solution.
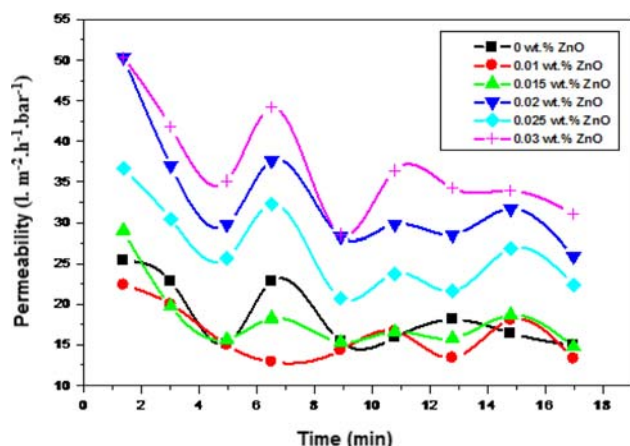
Fig. 9. Fw Direct red 80 solution permeability of PPSU membranes prepared from different ZnO nanoparticles.

membrane to 96.5 and 96.8% for the membranes prepared from 0.01 to 0.015 wt.% ZnO nanoparticles, respectively, whereas the rejection increases to 98.5 and 98.6% with an increase of ZnO nanoparticles to 0.02 and 0.025 wt.%, respectively. A further increase of the concentration of ZnO nanoparticles results in a decrease of the separation performance to 97.3%. It can be concluded that there is no significant reduction in rejection with addition of ZnO nanoparticles in the casting solution. Shen et al. [16] found that the rejection of the PES membrane is not significantly changed with addition of different compositions of the ZnO nanoparticles.

The time dependency of the flux of a dye solution through the PPSU membranes with different concentrations of ZnO nanoparticles in the casting solution is shown in Fig. 9. It can be seen that the PPSU membranes prepared from 0.02, 0.025, and 0.03 wt.% ZnO nanoparticles had a better performance than that of the neat membrane, and the steady state flux in comparison with the flux of the neat membrane was enhanced by 74, 50, and 109% with membranes prepared from 0.02, 0.025, and 0.03 wt.% ZnO nanoparticles, respectively.

The increased hydrophilicity of the PPSU membranes with addition of ZnO nanoparticles in casting solution results in a decrease of dye adsorption on the surface of the membrane due to the hydrophobic character of the dye. Therefore, the effect of membrane structure and hydrophilicity of the membranes on the rejection efficiency will be reduced. SEM images shown in Fig. 1 and the contact angles measured shown in Fig. 3 support this phenomenon.

4. Conclusions

(1)   SEM images illustrate that the PPSU membrane structure changes from a finger-like layer formed near the polyester support layer and a sponge-like layer formed near the top surface of the cross-section of the membrane prepared from neat PPSU to a fully sponge-like structure with increase of ZnO concentration in casting solution up to 0.025 wt.%. With a further increase in the ZnO concentration (i.e. 0.03 wt.%), the membrane morphology changes to a finger-like structure.

(2)   According to the AFM measurements, the PPSU/ZnO membranes containing nanoparticles up to 0.025 wt.% had a higher mean pore size and roughness. A further increase in the ZnO concentration to 0.03 wt.% results in a decrease of the mean pore size.

(3)   The membrane hydrophilicity increased with the increase of ZnO nanoparticle concentration in PPSU casting solution.

(4)   The pure water permeability of the PPSU membranes improved with the increase of the ZnO concentration up to 0.025 wt.%, whereas addition of 0.03 wt.% ZnO results in a decrease of the pure water permeability due to the morphological change and the reduction of the mean pore size. Moreover, similar results were observed using 0.02 and 0.025 wt.% ZnO nanoparticles in the casting solution due to the similar cross-sectional structure of the membranes.

(5)   There is no significant reduction in solute separation performance of the PPSU membranes with addition of ZnO nanoparticles in the casting solution.

References

[1]   D. Siavash, C. Johannes, T. Franco, T. Elena, L. Patricia, D. Jan, D. Enrico, B. Bart, Novel polyphenylsulfone membrane for potential use in solvent nanofiltration, J. Membr. Sci. 379 (2011) 60–68.
[2]   D. Siavash, T. Franco, C. Johannes, T. Elena, B. Fabio, B. Paola, L. Patricia, D. Jan, D. Enrico, B. Bart, Preparation of solvent stable polyphenylsulfone hollow fiber nanofiltration membranes, J. Membr. Sci. 384 (2011) 89–96.

[3] Anonymous, Design Guide for Radel Polymers, Solvay Advanced Polymers, Alpharetta, GA, USA, (2009). Available from: www.solvayadvancedpolymers.com.

[4] C. Xiaochun, M. Jun, S. Xuehua, R. Zhijun, Effect of TiO_2 nanoparticle size on the performance of PVDF membrane, Appl. Surf. Sci. 253 (2006) 2003–2010.

[5] S.J. Oh, N. Kim, Y.T. Lee, Preparation and characterization of $PVDF/TiO_2$ organic–inorganic composite membranes for fouling resistance improvement, J. Membr. Sci. 345 (2009) 13–20.

[6] L.Y. Yu, H.M. Shen, Z.L. Xu, PVDF–TiO2 composite hollow fiber ultrafiltration membranes prepared by TiO2 Sol–Gel method and blending method, J. Appl. Polym. Sci. 113 (2009) 1763–1772.

[7] R. Ahmad, J. Mohsen, R. Babak, R. Mostafa, TiO_2 entrapped nano-composite PVDF/SPES membranes: Preparation, characterization, antifouling and antibacterial properties, Desalination 278 (2011) 343–353.

[8] M. Khayet, J.P.G. Villaluenga, J.L. Valentin, M.A. Lo´pez-Manchado, J.I. Mengual, B. Seoane, Filled poly(2,6-dimethyl-1,4-phenylene oxide) dense membranes by silica and silane modified silica nanoparticles: Characterization and application in pervaporation, Polymer 46 (2005) 9881–9891.

[9] Y. Liang, J.S. Li, X.Y. Sun, L.J. Wang, Study of the microstructure of the nano Y-Al_2O_3/PVDF hollow fiber membrane, Technol. Water Treat. 30 (2004) 199–201.

[10] F. Liu, M.R. Moghareh Abed, K. Li, Preparation and characterization of poly(vinylidene fluoride) (PVDF) based ultrafiltration membranes using nano γ-Al_2O_3, J. Membr. Sci. 366 (2011) 97–103.

[11] I. Genné, S. Kuypers, R. Leysen, Effect of the addition of ZrO_2 to polysulfone based UF membranes, J. Membr. Sci. 113 (1996) 343–350.

[12] A. Bottino, G. Capannelli, A. Comite, Preparation and characterization of novel porous PVDF–ZrO_2 composite membranes, Desalination 146 (2002) 35–40.

[13] N. Maximous, G. Nakhla, W. Wan, K. Wong, Performance of a novel ZrO_2/PES membrane for wastewater filtration, J. Membr. Sci. 352 (2010) 222–230.

[14] Y. Chu, C. Wang, C. Chen, A new approach to hybrid CdS nanoparticles in poly(BA-co-GMA-co-GMA-IDA) copolymer membranes, J. Membr. Sci. 247 (2005) 201–209.

[15] S. Balta, S. Arcadio, L. Patricia, B. Lidia, B. Bart, J. Kim, A new outlook on membrane enhancement with nanoparticles: The alternative of ZnO, J. Membr. Sci. 389 (2012) 155–162.

[16] L. Shen, X. Bian, X. Lu, L. Shi, Z. Liu, L. Chen, Z. Hou, K. Fan, Preparation and characterization of ZnO/polyethersulfone (PES) hybrid membranes, Desalination 293 (2012) 21–29.

[17] J. Hong, Y. He, Effects of nano sized zinc oxide on the performance of PVDF microfiltration membranes, Desalination 302 (2012) 71–79.

[18] N. Jullok, S. Darvishmanesh, P. Luis, B. Van der Bruggen, The potential of pervaporation for separation of acetic acid and water mixtures using polyphenylsulfone membranes, Chem. Eng. J. 175 (2011) 306–315.

[19] Anonymous, The brochure of AO-Organic compounds, Acros Organics Part of Thermo Fisher Scientific, Geel, Belgium Available from: www.acros.com.

[20] Y. Yang, H. Zhang, P. Wang, Q. Zheng, J. Li, The influence of nano-sized TiO_2 fillers on the morphologies and properties of PSF UF membrane, J. Membr. Sci. 288 (2007) 231–238.

[21] S. Arcadio, A. Rashed, R. Zhang, A. Martínez, L. Braken, L. Patricia, B. Bart, Improved membrane structures for seawater desalination by studying the influence of sublayers, Desalination 287 (2012) 317–325.

[22] A. Bessieres, M. Meireless, R. Coratger, J. Beauvillain, V. Sanchez, Investigations of surface properties of polymeric membranes by near field microscopy, J. Membr. Sci. 109 (1996) 271–284.

[23] A. Idris, N.M. Zaina, M.Y. Noordin, Synthesis, characterization and performance of asymmetric polyethersulfone (PES) ultrafiltration membranes with polyethylene glycol of different molecular weights as additives, Desalination 207 (2007) 324–339.

[24] S. Rajesh, H. Kavalapara, A. Shobana, D. Mohan, Preparation, morphology, performance, and hydrophilicity studies of poly(amide-imide) incorporated cellulose acetate ultrafiltration membranes, Ind. Eng. Chem. Res. 50 (2011) 5550–5564.

[25] J. Li, Z. Xu, H. Yang, L. Yu, M. Liu, Effect of TiO_2 nanoparticles on the surface morphology and performance of microporous PES membrane, Appl. Surf. Sci. 255 (2009) 4725–4732.